In-situ Monitoring of the Interface Status and Ablation Depth in Ultrafast Laser Drilling

Tao Sun[1,2], Wanqin Zhao[*1,2], Zhengjie Fan[1,2], Jinge He[1,2], Jianlei Cui[1,2], and Xuesong Mei[1,2]

[1]*School of Mechanical Engineering, Xi'an Jiaotong University, China*
[2]*State Key Laboratory for Precision Micro-Nano Manufacturing Technologies, Xi'an Jiaotong University, China*
[*]*Corresponding author's e-mail: linazhao@xjtu.edu.cn*

Ultrafast laser processing is particularly well-suited for the processing of heterogeneous materials due to its advantages such as a wide range of materials applicability and high machining quality. However, the ablation depth has been difficult to control via the axial feed. In this situation, excessive damage and non-uniform ablation will occur in laser processing. In-situ monitoring and control of the machining process is one of the most promising methods to solve the problems. In this paper, we report an innovative method for in-situ monitoring of the interface status and ablation depth in ultrafast laser drilling of heterogeneous materials using optical coherence tomography (OCT). Firstly, the signal analysis and processing of the interference signal are developed for extracting the depth information. And then the interface detection of the heterogeneous materials and the measurement of the corresponding thickness before the drilling are demonstrated. Finally, the in-situ monitoring of the ablation depth is achieved. This study demonstrates the feasibility of utilizing spectral-domain optical coherence tomography (SD-OCT) for interface detection and in-situ monitoring of ablation depth in ultrafast laser drilling. The findings underscore the potential of SD-OCT in optimizing and achieving precise control of manufacturing processes.

1. Introduction

Heterogeneous materials are composed of two or more distinct materials or phases that are not uniformly distributed throughout the structure. Examples include composite materials, multilayered materials, and alloys, which are commonly used in aerospace, automotive, electronics, and medical devices [1, 2]. Due to its advantages such as wide range of materials applicability and high machining quality, ultrafast laser processing is well suited for the processing of heterogeneous materials [3, 4]. However, considering the propagation properties of Gaussian beam, the ablation depth has been difficult to control via the axial feed. In this situation, excessive damage and non-uniform ablation will occur in laser processing [5, 6], leading to the reduction of service life or even scrap of the workpiece. To address these challenges, in-situ monitoring and control of the machining process have become critical strategies in laser processing research [7]. In most studies, the in-situ monitoring of the machining process is achieved via laser-induced optical or acoustic emission, such as photodiode-based monitoring, spectrometer-based monitoring and acoustic-based monitoring [8, 9]. Yang et al presented an online spectrum monitoring system to achieve the interface sensing in laser processing of multilayer materials. The selective removal of a single layer can be realized [10]. However, the aforementioned methods rely on indirect information for monitoring the machining process. Their sensitivity to variations in machining parameters further hinders the development of accurate models for precise depth control [11].

Compared to indirect monitoring methods, direct monitoring can provide more intuitive information to understand and control the machining process. Lukas et al employed the high-speed synchrotron X-ray imaging to directly observe the dynamic formation and evolution of defects in real-time during laser percussion drilling, providing a basic understanding of the mechanisms and locations of defect formation [12]. In addition, other direct methods, such as laser-scanning confocal microscopy [13], ultrasound tomography [14], optical coherence tomography (OCT) [15], are applied for the in-situ monitoring of machining processes. Among them, OCT has attracted much attention for real-time monitoring and control of laser processing due to its advantages including high measurement resolution, wide measurement range, fast scanning speed and low cost [16]. Currently, OCT has demonstrated great potential in in-situ measurement of welding keyhole depth, laser ablation depth, and so on [17, 18]. Currently, only a few studies have investigated the application of OCT in detecting heterogeneous material interfaces and monitoring drilling depth. Conventional monitoring methods rely solely on spectral information to infer signal variations when the laser transitions to a different layer, but they cannot directly measure depth. Additionally, laser trepanning drilling is a spatiotemporally dependent process, where both machining position and drilling duration significantly influence the monitoring outcomes, adding complexity. Nonetheless, real-time monitoring of heterogeneous material interfaces and drilling depth during laser processing is crucial, warranting further investigation.

In this paper, the interface detection of heterogeneous materials and the measurement of the corresponding thickness are achieved via spectral-domain optical coherence tomography (SD-OCT) [19]. Furthermore, the spatial analysis of the in-situ measurement results at different positions is developed. Finally, the in-situ measurement of ablation depth is also demonstrated using the position-encoded scanning method. The rest of the article is organized as follows. In Section II, the experimental setup and methodology are introduced. Section III elaborates on the core aspects of this study, including OCT data processing, detection of heterogeneous material interfaces, and the realization of in-situ monitoring. Section IV summarizes the main conclusions.

2. Methodology

The schematic of the experimental system for in-situ monitoring and laser processing is shown in Figure. 1(b). The drilling experiments are carried out using the picosecond (ps) laser source (PX200-2-GF, Edgewave) delivering 10-ps pulses and up to 100W average power at 1030 nm. The SD-OCT can deliver detection light with a central wavelength of 840 nm, full width at half maximum (FWHM) of 45 nm. The axial resolution and depth measurable range are approximately 20.2 μm and 9.28 mm respectively. And the maximum line scanning frequency is 130 kHz for the SD-OCT, which enables rapid information acquisition during laser processing.
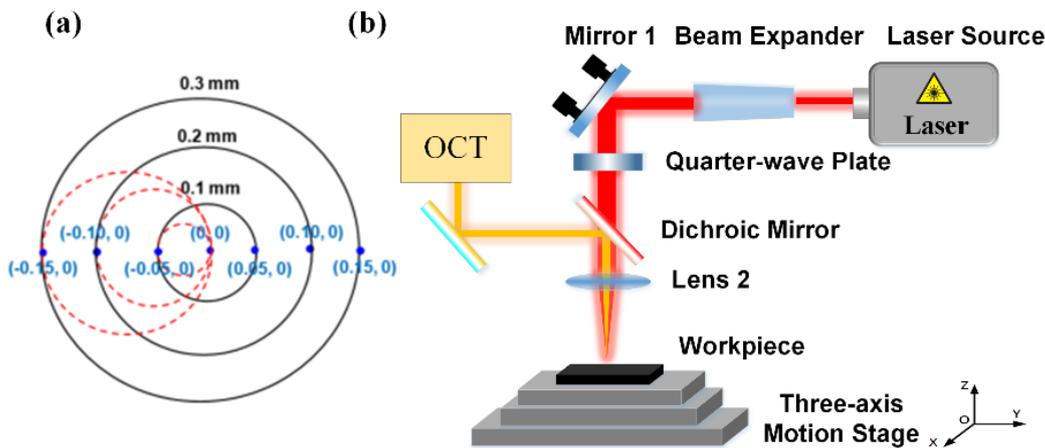
Fig. 1 Schematic of experimental setup for in-situ monitoring and laser processing. (a) The drilling trajectory and the set coordinate for position synchronous trigger. (b) Schematic of in-situ monitoring and laser processing system.

The ps laser and the sample beam of SD-OCT are coupled coaxially via a dichroic mirror (Thorlabs, DMLP950) and are focused onto the workpieces via an achromatic lens with a focus length of 125 mm. The relative motion between the workpieces and laser spot is controlled by a custom-built three-dimensional motion stage with a motion controller. For the in-situ monitoring experiment, a position synchronous scanning method is performed. When the motion stage reaches the set position, the SD-OCT will be triggered to acquire the corresponding depth information. Thus, the depth information and corresponding coordinate can be obtained simultaneously.

As shown in Figure. 1(a), the drilling trajectory is concentric circle, which is used to achieve the laser trepanning drilling. The black line indicates the drilling trajectory with the laser ablation and these blue dots are the set positions for the position-synchronous trigger. And the red dashed line indicates the secondary trajectory without the laser ablation, which is used to ensure velocity continuity during coordinate jump. The material is a multilayer heterogeneous structure consisting of a thermal barrier coating (TBCs), a bonding coat (BC) layer, and a GH4169 superalloy. Since neither the superalloy layer nor the BC layer exhibits optical transparency, they are treated as a single material category during in-situ measurement. The scanning electron images were obtained using a scanning electron microscopy (SEM, Hitachi, S3000H) and the cross-profile of the hole was observed by an X-ray 3D microscope (XRM, Zeiss, Xradia 610versa).

3. Results and Discussion

3.1 Signal processing and depth extraction

According to the Wiener-Khinchin theorem, the power spectral function $S(k)$ of the light source and its autocorrelation function $\gamma(z)$ are a pair of Fourier transforms. Thus, the interference signal can be described as follows based on Fourier transform and its convolution properties [20].

$$I_D(k) = \frac{\rho}{8}[\gamma(z)[R_R + R_{S_1} + R_{S_2} + ...]]$$

$$+ \frac{\rho}{4}\sum_{n=1}^{N}\sqrt{R_R R_{Sn}}[\gamma[2(z_R - z_{Sn})] + \gamma[-2(z_R - z_{Sn})]] \quad (1)$$

$$+ \frac{\rho}{8}\sum_{n \neq m=1}^{N}\sqrt{R_{Sn} R_{Sm}}[\gamma[2(z_{Sn} - z_{Sm})] + \gamma[-2(z_{Sn} - z_{Sm})]],$$

where ρ indicates the responsivity of the detector, A/W; R_R is the reflectivity of the mirror in the reference arm; $R_{Sn}(n=1,2,3,...)$ represents the reflectivity of the sample at different depths; $z_{Sn}(n=1,2,3,...)$ indicates the optical path difference between the beam splitter and the mirror in the reference arm, mm; And $z_{Sm}(m=1,2,3,...)$ indicates the optical path difference between the beam splitter and different depths in the sample, mm.

The result in Eq. 1 consists of three distinct components: (1) Direct current (DC) component, which is independent of the optical path and whose intensity depends on the power reflectivity of the reference mirror and the sum of the sample reflectivity. (2) Cross correlation (CC) component. The

component indicates the interference between the reflected/scattered light from the sample at different depths and the reference light. Decoding this component enables the extraction of depth information. (3) Auto correlation (AC) component. The interference between the reflected/scattered light from the sample at different depths are encoded in this component, which has minimal impact on the measurement result. However, some unnecessary noise is present. Thus, signal processing is required to extract the depth information. In general, signal processing includes background subtraction, k-domain linearization, and fast Fourier transform (FFT) [21]. Fig. 2 illustrates the optical interference signal, along with a comparison of its Fourier transform before and after data processing.

3.2 Detection of interface status

As mentioned above, the CC component includes the interference between the reflected/scattered light from the sample at different depths and the reference light. As shown in Fig. 3(a), for the two-layer heterogeneous materials (ceramic and metal layer), there are two interfaces: the air-ceramic interface and the ceramic-metal interface. In this case, the first reflection occurs when the detection light is transmitted to the air-ceramic interface. And the second reflection takes place when the light is incident on the ceramic-metal interface. As shown in Eq. 1, the intensity of the CC component depends on the reflectivity of the sample at different depths. Thus, interface detection can be easily achieved.

Fig. 3(b) shows the results measured by SD-OCT. It can be observed that there are two peaks in the measurement result, which represent different interfaces, respectively. According to the results, the thickness of the ceramic layer can be obtained, which is consistent with the results measured by SEM. The deviation is 23.7 µm. On the one hand, this deviation may arise from measurement errors at different locations, likely due to variations in the ceramic layer thickness or the influence of the BC layer. On the other hand, it may stem from dispersion broadening or mismatch during laser transmission within the ceramic. These factors warrant further investigation to enhance the accuracy of measurements.

3.3 In-situ monitoring of the ablation depth.

Nevertheless, there are some problems when the OCT is applied for in-situ monitoring of laser trepanning drilling. In general, the scanning mode of OCT is linear scanning. OCT itself can only measure in depth information. After brightness scan (B-scan), the depth information can be formed into a two-dimensional image, and multiple two-dimensional images can be reconstructed into a three-dimensional volume [22]. This is why OCT is currently mainly used in some processing applications based on linear scanning mode. However, the trajectories are circular in laser trepanning drilling. It's difficult to determine the corresponding position for in-situ depth measurement.
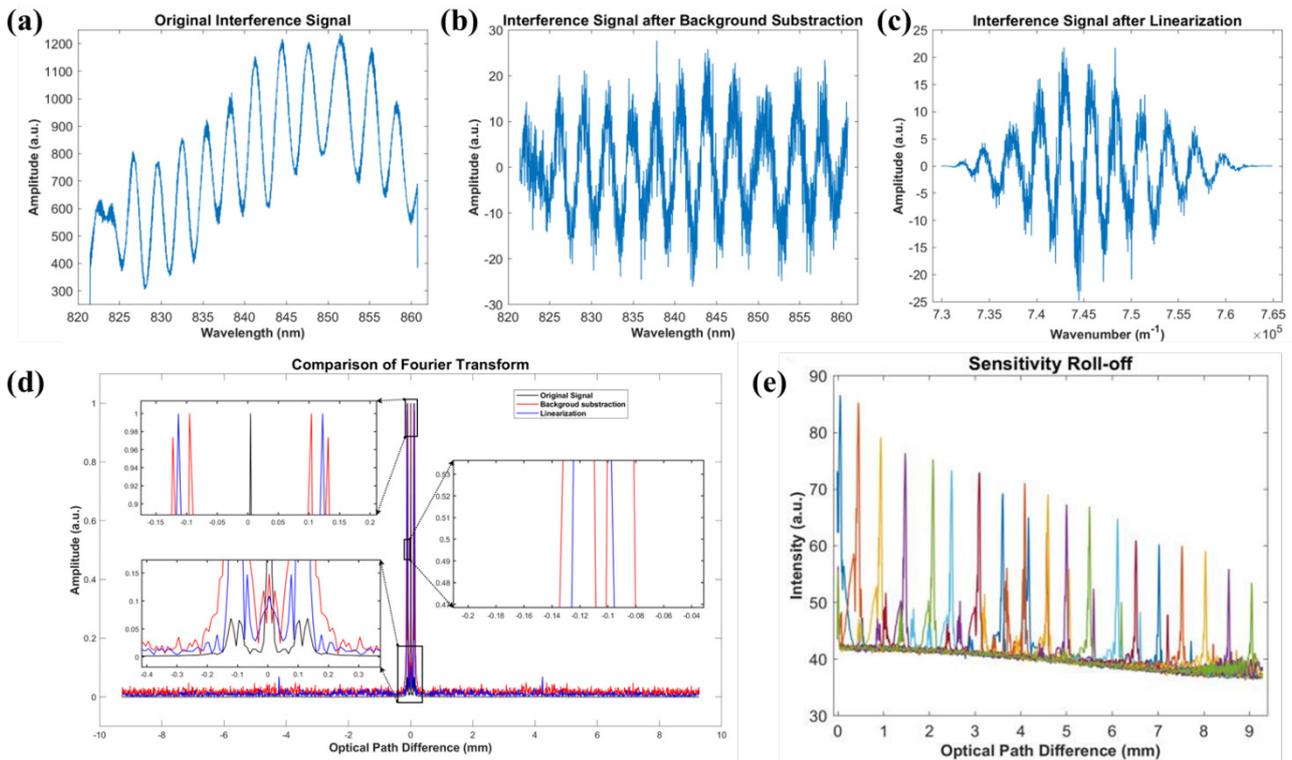
Fig. 2 Optical interference signal and the comparison of its Fourier transform. (a) Original interference signal; (b) Interference signal after background subtraction; (c) Interference signal after linearization; (d) Comparison of Fourier transform before and after signal processing; (e) Change in signal intensity of the Fourier spectrum versus the OPD.
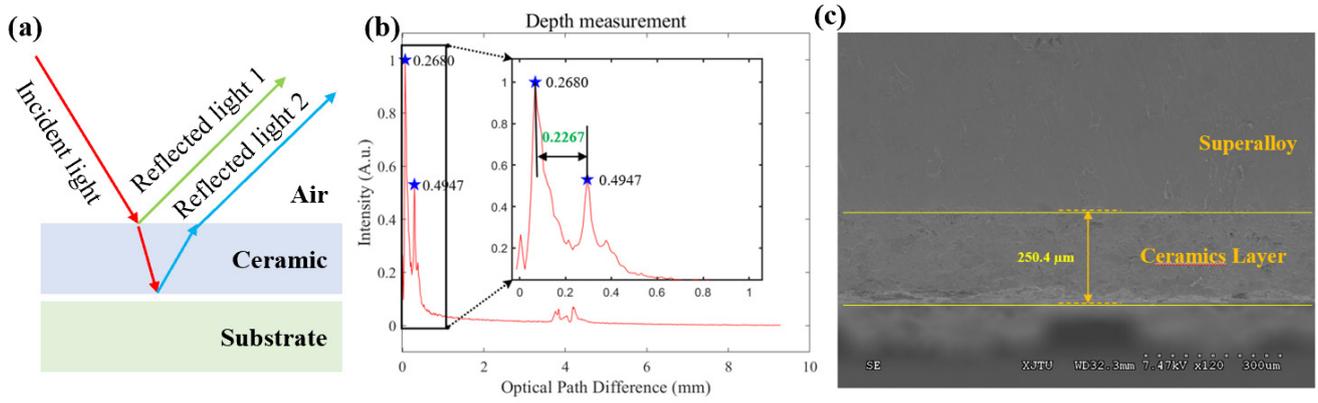
Fig. 3 Principle and results of the interface detection using OCT. (a) Principle of the interface detection for two-layer heterogeneous materials; (b) Interface detection and thickness measured by OCT; (c) Thickness of the ceramics layer measured by SEM.

Thus, we develop a position synchronous scanning method for in-situ depth measurement during laser trepanning drilling. First, the target positions for synchronization are predefined. By leveraging the real-time position feedback from the motion stage, the controller compares the current positions with the target positions. Once the feedback position reaches the predefined target, a signal is generated to trigger the OCT device, thereby achieving position-synchronized scanning.

However, due to the complex machining phenomenon, such as multiply reflections, debris ejection and so on, there are some differences between the measurement results in different positions. Thus, it's necessary to identify the spatial correlation between the measurement results and the position. To reduce the complexity of the experiment, the workpiece is changed into stainless steel. Fig. 4 demonstrates the measurement results in different positions. It can be found that there are larger differences between the measurement results. These differences are primarily attributed to factors related to laser energy distribution and trajectory overlap. Firstly, the Gaussian energy distribution of the laser beam results in higher energy density in the central regions of the beam, causing inner-circle regions to experience more effective ablation. Similar to percussing drilling, a conical hole is inevitably formed even in the absence of any movement [23]. Secondly, the shorter or more repetitive scanning paths in inner-circle regions lead to increased pulse overlap, thereby delivering a higher total energy to these areas [24]. Thus, the materials in the inner circle will be ablated more quickly.

This is also why the measurement value is larger at (0.05,0) and (-0.05, 0). On the other hand, as displayed in Fig. 4(c) the debris existing inside the hole will also influence the measurement results. Thus, there are different measurement values even at the same coordinates. Anyway, it can be observed that the measured depth at the coordinate (0.05, 0) is consistent with the hole depth measured by XRM. The deviation of 44 µm is sufficiently small relative to the sample thickness and the OCT system's inherent precision, demonstrating the efficacy of OCT in in-situ monitoring of ablation depth. This deviation might result from interference caused by scattering particles during the machining process or the deposition of debris within the hole. Further investigation is needed to elucidate these mechanisms.

4. Conclusions

In conclusion, we report an innovative method for in-situ monitoring of the interface status and ablation depth in ultrafast laser drilling using optical coherence tomography (OCT). The experimental system for in-situ monitoring and laser processing is established and the corresponding data processing algorithm is developed. Then the interface detection and thickness measurement of the two-layer heterogeneous material are achieved via the above method. The measurement deviation is 23.7 µm. Finally, the spatial correlation between the measurement results and the spatial coordinates is simply analysed. There are large differences between the measurement results in different positions and
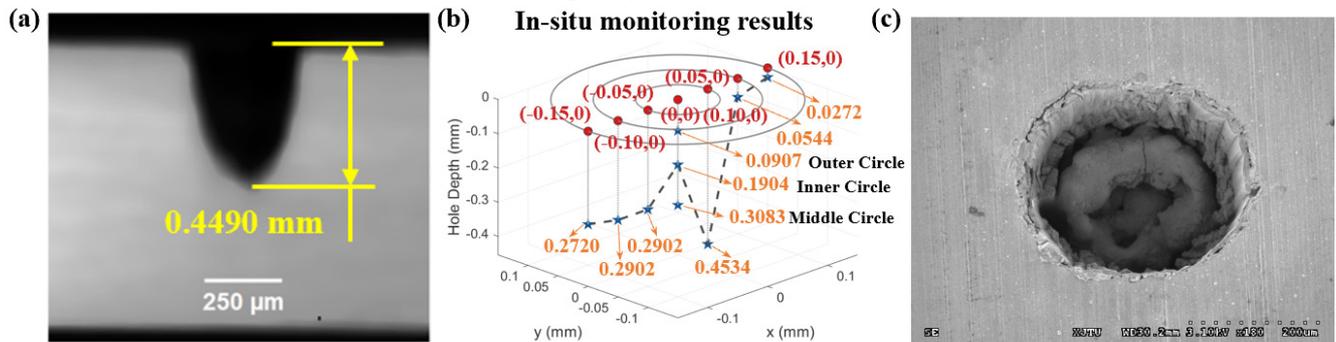
Fig. 4 Verification of the in-situ monitoring results. (a) Cross-section profile and the depth of the drilled hole; (b) In-situ monitoring results at different drilling positions; (c) Debris deposition inside the hole.

the result at coordinate (0.05, 0) is most consistent with the actual hole depth. This study fully presents the feasibility of SD-OCT in interface detection and in-situ monitoring of ablation depth in ultrafast laser drilling, which has wide potential in optimizing and realizing accurate control of the manufacturing process. In the future, the effect of the hole evolution process on in-situ monitoring using OCT should be further investigated and the closed-loop control technologies based on the OCT should be further developed.

Acknowledgments and Appendixes

References

[1] G. Y. Yang, Y. H. Ding, L. Liu, H. Z. Yang, X. Q. Wu, W. Xiong, and L. M. Deng: J. Mater. Process. Technol., 312, (2023) 117868.

[2] Z. Xu, L. Jiang, S. Wang, J. Sun, J. Zhan, and W. Zhu: Spectrochim Acta, Part B, (2024). 107088.

[3] X. M. Sun, X. Dong, K. D. Wang, P. F. Fan, T. Sun, X. S. Mei, and Z. J. Fan: Opt. Laser Technol., 170, (2024) 110201.

[4] P. Shen, X. M. Mei, T. Sun, X. S. Zhuo, X. M. Sun, W. j. Wang, and Z. J. Fan: Prog. Nat. Sci.:Mater. Int., 34, (2024) 942.

[5] T. Sun, X. S. Mei, X. M. Sun, Y. X. Cai, Y. C. Ji, and Z. J. Fan: IEEE Trans. Ind. Inform., 19, (2023) 5422.

[6] G. Chang and Y. L. Tu: Int. J. Mach. Tools Manuf., 60, (2012) 35.

[7] T. Sun, Z. J. Fan, X. M. Sun, Y. C. Ji, W. Q. Zhao, J. L. Cui, and X. S. Mei: J. Manuf. Process., 101, (2023) 990.

[8] K. Wasmer, T. L. Quang, B. Meylan, F. V. Farahani, M.P. Olbinado, A. Rack, and S. A. Shevchik: Procedia CIRP., 74, (2018) 654.

[9] Q. R. Zhang, X. N. Zhang, Y. L. Zhou, Y. Hai, B. Wang, and Y. C. Guan: J. Manuf. Process., 117, (2024) 224.

[10] G. Yang, Y. Ding, L. Liu, H. Yang, X. Wu, W. Xiong, and L. Deng: J. Mater. Process. Technol., 312, (2023) 117868.

[11] C. C. Ho, Y. J. Chang, J. C. Hsu, C. M. Chiu, and C. L. Kuo: Measurement, 80, (2016) 251.

[12] L. Schneller, M. Henn, C. Spurk, M. Hummel, A. Olowinsky, F. Beckmann, and T. J. Graf: J. Laser Micro Nanoeng., 19, (2024) 151.

[13] X. Chen, Y. Xu, N. K. Chen, S. Shy, and H. C. Chui: Photonics, 8, (2021) 493.

[14] M. S. Sutopa, T. Sultan, E. H. Rozin, and C. Cetinkaya: J. Manuf. Process., 101, (2023) 1188.

[15] J. Zhao, C. Zhang, Y. Ding, L. Bai, and Y Cheng: Photonics, 11, (2024) 743.

[16] D. Huang, E. A. Swanson, C. P. Lin, J. S. Schuman, W. G. Stinson, W. Chang, M. R. Hee, T. Flotte, K. Gregory, C. A. Puliafito, and J. G. Fujimoto: Science, 254, (1991) 1178.

[17] S. Hasegawa, M. Fujimoto, T. Atsumi, and Y. Hayasaki: Light Adv. Manuf., 3, (2022) 427.

[18] T. G. Fleming, S. J. Clark, X. Q. Fan, K. Fezzaa, C.L. A Leung, P. D. Lee, and J. M. Fraser: Addit. Manuf., 77, (2023) 103798.

[19] J. F. De Boer, R. Leitgeb, and M. Wojtkowski: Biomed. Opt. Express, 8, (2017) 3248.

[20] X. S. Mei, T. Sun, W. Q. Zhao, Z. J. Fan, T. Zhang, C. Tang, J. L. Cui, and W. J. Wang: J. Mech. Eng., 59, (2023) 216.

[21] N. Liu, C. X. Dai, Y. H. Tang, and P. Xi: J. Innov. Opt. Health. Sci., 07, (2014) 1450031.

[22] A. Aumann, S. Donner, J. Fischer, and F. Muller: "Optical coherence Tomography (OCT): Principle and Technical Realization", ed. By Springer Cham (Publisher, Switzerland, 2019), p.61.

[23] W. Q. Zhao, X. S. Mei, and L. Z. Wang: Ceram. Int., 48, (2022) 36297.

[24] K. M. Abedin, D. W. Coutts, and C. E. Webb: Appl. Phys. A, 78, (2004) 737.